Design and Implementation of Battery Management System Using Passive Cell Balancing, interfacing with Blynk IoT

Gopalasetti Jaganmohana Rao [1], Racharla Venkateswarlu [2] Dr. T.R. Jyothsna[3]
[1,2,3] *Department of Electrical Engineering, Andhra University College of Engineering, Visakhapatnam, Andhra Pradesh, India*

Abstract: Battery Management Systems (BMS) are pivotal for the safety, efficiency, and lifespan of Lithium-ion (Li-ion) batteries in electric vehicles (EVs) and energy storage systems. This work details the design and practical implementation of a BMS employing passive cell balancing and Blynk IoT-based interfacing for real-time monitoring and control. The system architecture integrates a boost converter, managed by an Adaptive Sliding Mode Controller (ASMC) through MATLAB/Simulink modeling. For hardware realization, ESP32 serves as the main controller, coordinating with sensors (ADS1115, INA219, DHT11, flame sensor) and actuators (relay modules) to achieve automatic cell balancing and protective functions. Wireless connectivity via Blynk IoT enables remote observation and management of battery parameters, enhancing system intelligence and user accessibility. Experimental results confirm that the proposed approach provides efficient cell balancing, robust protection, and high reliability for battery storage applications.

Keywords-Battery Management System (BMS), Adaptive Sliding Mode Controller (ASMC), Lithium-ion Battery (Li-ion), Electric Vehicles (EVs), Blynk IoT, ESP32, MATLAB/Simulink.

I. INTRODUCTION

Battery Management Systems (BMS) are essential for ensuring the safety, efficiency, and operational lifespan of Lithium-ion battery packs deployed in electric vehicles and energy storage applications. This research presents the development and implementation of a BMS utilizing passive cell balancing and real-time IoT monitoring via Blynk, integrating ESP32 hardware and sensors for automated protection and system reliability.

The proposed system architecture features a boost converter regulated by an Adaptive Sliding Mode Controller (ASMC)modelled in MATLAB/Simulink, allowing precise battery charging and balancing control. Wireless Blynk connectivity enables remote battery parameter management, and experimental results validate the solution’s effectiveness in achieving efficient cell balancing, protection, and robust performance for advanced battery storage systems.

II. METHODOLOGIES AND MODELLING

Cell balancing is critical in battery packs, especially lithium-ion types, to maintain uniform state of charge (SOC) and voltage across individual cells. Unequal cell voltage or SOC reduces battery efficiency, lifetime, and safety. Cell balancing techniques are generally classified into two main categories: passive balancing and active balancing.

A. Passive Cell Balancing:

- Passive balancing equalizes cell voltage by dissipating excess energy from higher-charge cells as heat via resistors.
- It is simple and low cost but inefficient due to energy loss.
- Methods include fixed shunting resistors and switching shunting resistors.
- Generally used during charging mode and suitable for battery packs with low current requirements.
- Drawbacks include energy wastage and increased thermal management needs.

B. Active Cell Balancing:
Active Balancing Simulation Results:

- Energy redistributed from higher SOC cells to lower SOC cells using converter or capacitor-based circuits.

- Higher efficiency: minimal energy lost as heat compared to passive methods.
- Faster equalization of cell voltages and SOC; balancing current maintained throughout the process.
- Efficient balancing observed both during charging and discharging cycles.

C. Mathematical Model of Boost Converter with Adaptive Sliding Mode Controller:

The DC-DC boost converter plays a vital role in Electric Vehicle (EV) battery charging systems by stepping up the input voltage to the required battery charging voltage level. For a 4-cell Li-ion battery pack, efficient charging requires precise voltage regulation, robustness to load changes, and adaptability to system disturbances. The use of Adaptive Sliding Mode Control (ASMC) provides high stability, fast dynamic response, and reduced chattering compared to conventional control methods. A boost converter consists of an inductor, a switch (MOSFET), a diode, and an output capacitor. The key governing equations in continuous conduction mode (CCM) are derived from following circuit diagram.

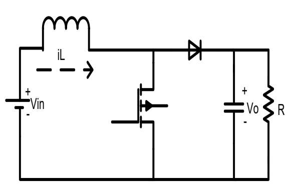

Figure 1: Boost converter circuit

1. Inductor voltage equation:

$$L\frac{di_l}{dt} = V_{in} - (1-d)V_O \quad (1)$$

2. Output capacitor voltage equation:

$$C\frac{dVo}{dt} = (1-d)i_l - \frac{V_o}{R} \quad (2)$$

3. The output voltage gain:

$$V_O = \frac{V_{in}}{(1-d)} \quad (3)$$

These equations from the basis for controller design in MATLAB Simulink.

Design of Adaptive Sliding Mode Controller (ASMC):

Sliding Mode Control (SMC) works by forcing the system states to "slide" along a predefined surface until the desired output is reached.

In ASMC, the controller parameters adapt dynamically based on system error, ensuring robustness under parameter variations.

Under continuous conduction mode, the averaged model of the converter is:

$$\dot{x}_1 = \frac{di_l}{dt} = V_{in} - (1-d)V_o \quad (4)$$

$$\dot{x}_2 = C\frac{dVo}{dt} = (1-d)i_l - \frac{V_o}{R} \quad (5)$$

Estimator based Adaption Law Design:

x_1 and x_2 are assumed to be accessible.

An estimator is used to facilitate the design of parameter adaption laws for $\hat{\theta}$ and $\hat{V}_{in}$

Estimator is considered as:

$$\dot{\hat{x}}_1 = -(1-\mu)\frac{\hat{x}_2}{L} + \frac{\hat{V}_{in}}{L} + K_1(x_1 - \hat{x}_1) \quad (6)$$

$$\dot{\hat{x}}_2 = (1-\mu)\frac{\hat{x}_1}{C} - \frac{\hat{\theta}}{C}x_2 + K_2(x_2 - \hat{x}_2) \quad (7)$$

The adaption laws are determined by cancelling the terms in brackets and given by

$$\dot{\hat{\theta}} = -\gamma_1 x_2 \tilde{x}_2 \quad (8)$$

$$\dot{\hat{V}}_{in} = \gamma_2 \tilde{x}_1 \quad (9)$$

Adaptive SMC design:

1. Switching surface

$$S = \hat{x}_1 - \frac{V_{ref}^2}{\hat{V}_{in}}\hat{\theta} \quad (10)$$

2. Control law:

$$\mu_{eq} = 1 - \frac{(\hat{V}_{in} + K_1 L\tilde{x}_1 + \frac{\gamma_1 L V_{ref}^2}{\hat{V}_{in}} x_2\tilde{x}_2 + \frac{\gamma_2 L V_{ref}^2}{\hat{V}_{in}^2}\hat{\theta}\tilde{x}_1)}{\hat{x}_2} \quad (11)$$

III. SIMULATION RESULTS

A. Passive Cell Balancing System:

The simulation models the behaviour of a lithium-ion battery pack comprising multiple series-connected cells, each monitored for state of charge (SOC), current, and voltage. The system architecture reflects individual cell measurement modules, passive balancing circuits using resistors and MOSFETs, and a centralized control unit for data processing and balancing command execution.

Functional Components:
Cell Measurement Units, Passive Balancing Circuits
Centralized BMS Logic, Monitoring and Display

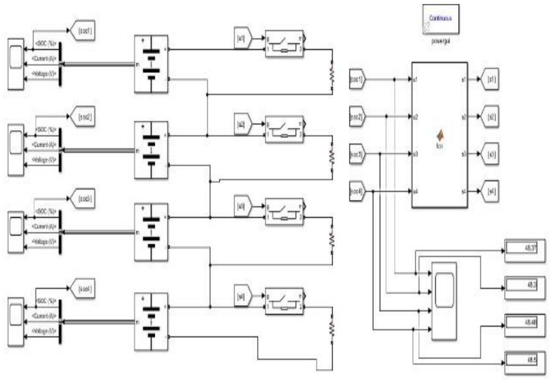

Figure 2: Passive cell balancing Simulink diagram

The results section should detail the following:
Initial cell voltages and SOC distribution before balancing, demonstrating imbalance conditions.
Activation of balancing circuits based on controller decisions, with time-stamped events illustrating the reduction of voltage disparities across cells.
Final cell voltages (e.g., measurements such as 48.37V, 48.3V, 48.48V, 48.5V) showing alignment and improved battery health after the balancing process.

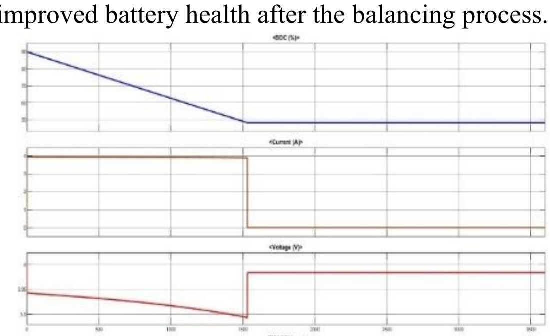

Figure 3: Results of Cell Parameters

State of Charge (SOC), Current, and Voltage Trends: Figure 3 displays the SOC (%), current (A), and voltage (V) profiles for individual cells throughout the balancing process. Initially, the cells exhibit different SOC and voltage levels, indicating imbalance. When passive cell balancing is activated, the system equalizes the SOC and voltage values, as seen by the convergence of the traces after the balancing event occurs around the 1500-second mark. Current profiles show active balancing, followed by stabilization when the cells reach uniform SOC.

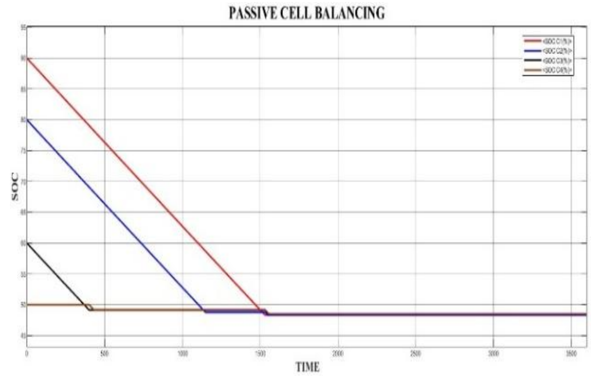

Figure 4: Results of State of Charge (SOC) of each cell for passive balancing

Passive Cell Balancing Convergence: Figure 4 provides a focused view on SOC for four different cells over time under passive balancing. Each coloured line represents a specific cell's SOC. At the beginning, distinct SOC values signify imbalance, with more charged cells decreasing in SOC faster as energy is dissipated through the passive balancing circuit. After approximately 1500 seconds, all cell SOCs converge to nearly identical values, confirming the effectiveness of the passive technique in achieving optimal balance.

Interpretation
These results validate the designed passive cell balancing system:
SOC and voltage disparities are eliminated efficiently within a short time frame.
The controller effectively detects imbalance, activates the necessary balancing circuits, and deactivates them once all cells reach equilibrium.
The final values across all cells demonstrate enhanced pack stability and readiness for further charge/discharge cycles under safe, reliable operation.
These findings substantiate the robustness and efficiency of your proposed battery management solution.

B. Active Cell balancing:
The active cell balancing system is designed and simulated in Simulink. The simulation model consists of the following major blocks:
Battery Pack Model, Cell Voltage Monitoring, Balancing Algorithm, Controller Design.

Simulation Parameters:
Simulation time: 0–2000 seconds.
Nominal cell capacity: 2.5 Ah.
Initial SOC imbalance introduced.
Switching frequency: 50 kHz.

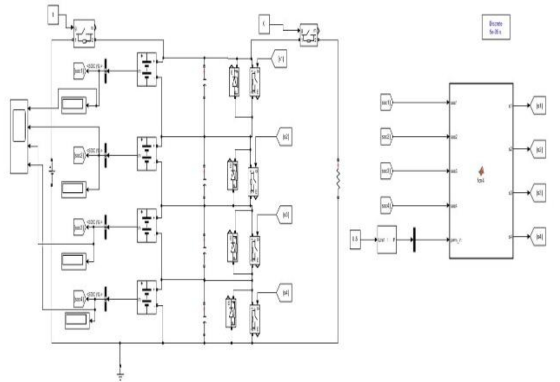

Figure 5: Simulink diagram of Active cell balancing.

The results of the MATLAB/Simulink simulation validate the effectiveness of the proposed active cell balancing system.

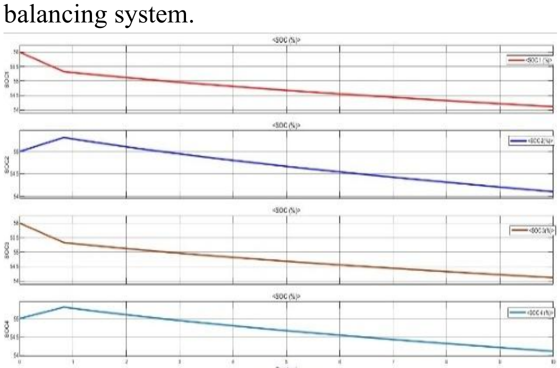

Figure 6: Results of State of Charge (SOC).

SOC Convergence:
The SOC of the individual cells was observed to gradually equalize. The difference between the maximum and minimum SOC reduced significantly after balancing, demonstrating efficient energy redistribution.

C. Boost Converter with Adaptive Sliding Mode Controller:

The MATLAB Simulink model consists of:
Boost converter circuit: inductor, MOSFET switch, diode, capacitor, and load.
PWM generator: producing gate signals based on ASMC duty cycle.
ASMC block: receives feedback, calculates error, updates sliding surface, and adjusts duty cycle.
Measurement blocks: monitoring, duty cycle, and switching frequency.

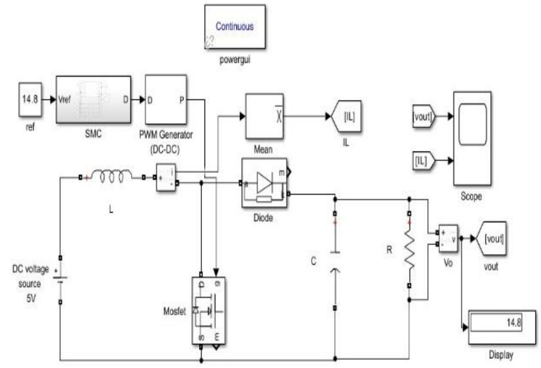

Figure 7: Boost converter with Adaptive sliding mode control Simulink diagram

This section presents the MATLAB/Simulink simulation results for the designed DC–DC boost converter, which steps up the input voltage from 5 V to 14.8 V for charging a series-connected Li-ion battery pack. The converter was designed using the calculated parameters:
Inductor (L): (11.82 µH), Output Capacitor (C): (25.1 µF), Load Resistance (R): 30 Ω
Switching Frequency: 50 kHz

Output Voltage Performance
The simulated output voltage waveform is shown in Figure 7.
The converter successfully boosts the 5 V input to the desired 14.8 V output. The voltage reaches steady-state within approximately 3–4 ms and remains stable with a ripple of about 20 mV.

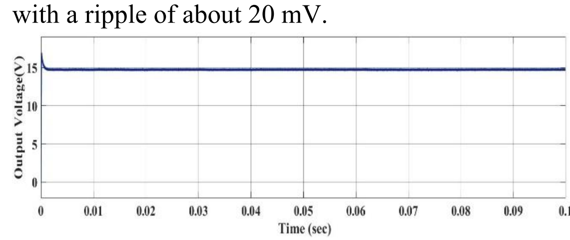

Figure 8: Boost converter Output Voltage Vs Time graph

Observation:
The voltage ripple is well within the safe charging limits for Li-ion batteries, ensuring stable charging without overshoot or oscillations.

Inductor Current Performance:
The inductor current waveform is shown in Figure 8. The current rises during the switch ON period and falls

during the OFF period, exhibiting continuous conduction mode (CCM) operation.

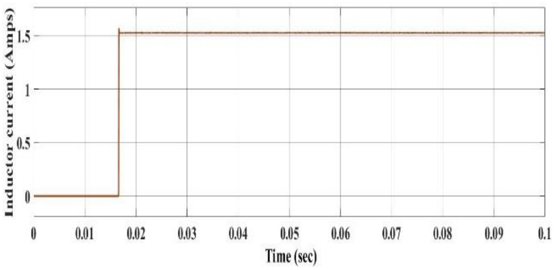

Figure 8: Boost converter Inductor current Vs Time graph

Observation:
The peak inductor current is approximately
1.55 A, with a ripple of around 0.10 A (≈ 6.8 % of the average current). This ripple is within the acceptable design limits, preventing excess heating or core saturation.

Discussion:
The simulation confirms that the selected component values allow the boost converter to achieve the desired output voltage while maintaining low ripple in both voltage and current. The fast-settling time ensures efficient and stable battery charging, which is particularly important for Li-ion chemistry.

IV. HARDWARE IMPLEMENTATION OF PASSIVE CELL BALANCING BMS

The proposed Passive Cell Balancing Battery Management System (BMS) is designed for a 4-cell Li-ion battery pack. The overall architecture integrates sensing modules, a control and processing unit, balancing circuitry, protection components, display feedback, IoT connectivity, and load/cooling control mechanisms. The block diagram of the system is shown in Figure 9.

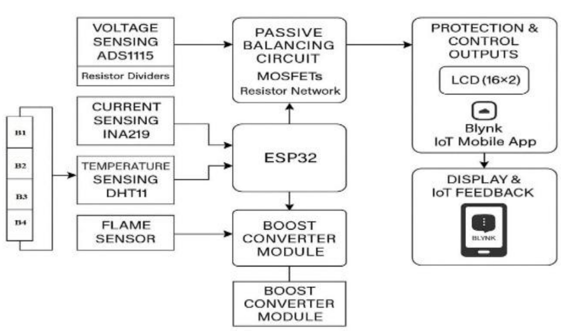

Figure 9: Block Diagram of the BMS.

Circuit Design:
The passive balancing circuit used in this project is implemented separately for each of the four cells in the battery pack.
1. N-channel MOSFETs (one per cell) — control the balancing action by switching the resistor load in and out.
2. Bleed Resistors — chosen to provide the required discharge current while keeping heat dissipation manageable.
3. Control Signals from ESP32 — generated based on real-time voltage readings from the ADS1115.

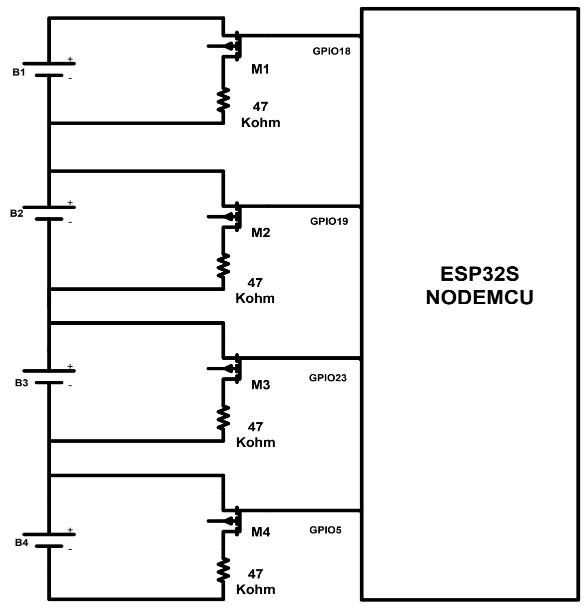

Figure 10: Circuit diagram of passive cell balancing.

LCD Display Integration:
The 16×2 I²C LCD is directly connected to the ESP32S via the I²C protocol (SDA and SCL lines), which reduces wiring complexity and uses only two GPIO pins. The LCD provides real-time visual feedback of the following parameters:
Cell voltages (C1, C2, C3, C4), SOC, SOH, Battery temperature (from DHT11 sensor)

Blynk IoT Integration:
The Blynk IoT platform is used to transmit BMS data to a cloud server, enabling real-time monitoring and control from any location using a smartphone app. The ESP32S connects to Wi-Fi and sends parameters such as:
Cell voltages (V1–V4 in Blynk app), Current (from INA219 sensor), Temperature (from DHT11).

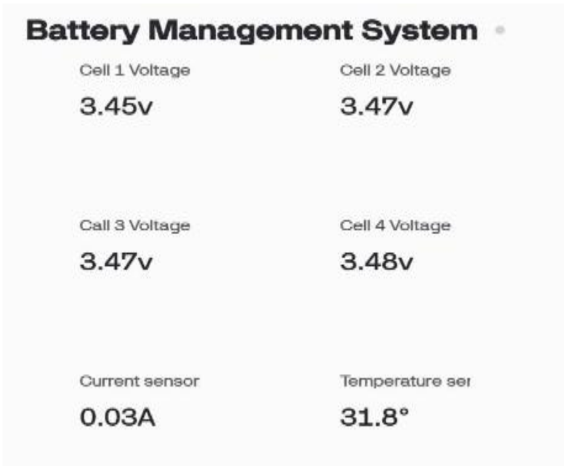

Figure 11: Blynk IoT Integration with ESP32S

Summary of Test Results:
The implementation confirmed that:

- The passive balancing circuit effectively reduced cell voltage differences.
- Alerts were triggered accurately and immediately upon threshold violations.
- The LCD and Blynk app provided clear, real-time feedback.

The hardware system responded reliably to changes in voltage, temperature, and fire detection sensors.

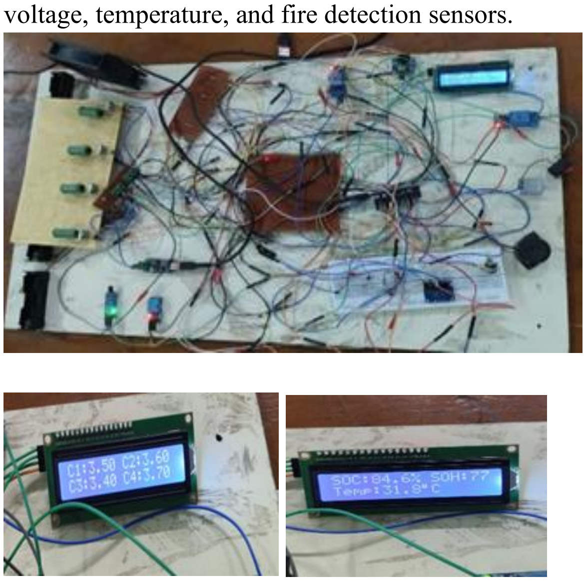

Figure 12: Hardware implementation of passive cell balancing

Key observations:
Balancing started only when the voltage threshold and imbalance conditions were met.
Only the cell with the highest voltage was targeted at a time.
The balancing current was determined by the resistor value (calculated for safe dissipation).

V. RESULTS, DISCUSSION, CONCLUSION, AND FUTURE SCOPE

A. Comparison: Passive and Active Cell balancing simulations and Hardware Results of Passive Balancing:
Passive Balancing Simulation Results:
Passive balancing triggered for cells with SOC higher than the pack average by >0.02.
Balancing current gradually reduced as all cells approached uniform voltage.
Energy loss observed as heat in shunt resistors during balancing.
Balancing predominantly active during charging; slower to equalize cells relative to active balancing.

Active Balancing Simulation Results:
Energy redistributed from higher SOC cells to lower SOC cells using converter or capacitor-based circuits.
Higher efficiency: minimal energy lost as heat compared to passive methods.
Faster equalization of cell voltages and SOC; balancing current maintained throughout the process.
Efficient balancing observed both during charging and discharging cycles.

Passive Balancing Hardware Results:
MOSFET-based balancing circuits effectively reduced SOC disparity in high SOC cells.
Voltage deviation between cells decreased from <50 mV to <10 mV during charging.
Slight current variation observed due to component tolerances (resistors, MOSFETs).
Successful practical implementation, though balancing speed and energy efficiency lag behind active schemes.

B. Challenges Faced and Solutions:
Sensor Calibration: INA219 and ADS1115 readings initially inaccurate; resolved via offset correction in code.

Noise in Voltage Readings: Reduced by adding filtering capacitors and implementing a moving average in firmware.

MOSFET Heating in Balancing: Managed by using higher wattage resistors and heat sinks.

Wi-Fi Connectivity Drops: Replaced Blynk.begin() with non-blocking Blynk.config() and Blynk.connect().

C. Future Scope: Full Integration of Converter and BMS:
Integration of the boost converter control directly into the BMS firmware to allow dynamic voltage adjustment based on SOC and temperature.

D. Real-World EV Application
Testing Deploy the system in an electric two-wheeler for field testing. Gather long-term performance data on battery health, thermal stability, and energy efficiency.

E. Conclusion: The developed ESP32-based BMS with ASMC-controlled boost converter meets the requirements for safe, reliable, and efficient charging of a 4-cell Li-ion battery pack. Both simulation and hardware tests validate the system's performance, making it suitable for integration into small electric vehicle applications.

REFERENCE

[1]. In Rui Hu's (2011) thesis," Battery Management System for Electric Vehicle Applications" was published at the University of Windsor.

[2]. Jerin Miller's (2012) thesis," Minimization of Circuitry in Large Format Lithium-Ion Battery Management Systems," has been proposed.

[3]. Georgios Darikas' (2018) thesis," Design and Implementation of a Battery Management System for Lithium-Ion Batteries suitable for Automotive Applications," has been proposed.

[4]. Hariprasad et al. (2020) thesis," A comprehensive study on lithium-ion battery management system," has been proposed.

[5]. Eriksson & Nilsson's (2018) thesis," Battery Management System (State of Charge Estimation)," has been proposed.

[6]. Dr Eseosa Omorogiuwa & Kingsley Nnaemeka Eze (2020) "A comprehensive study on lithium-ion battery management system" has been proposed.

[7]. Floridia Stefano & Passerone Claudio (2021-22) "Analysis and development of Battery Management System for electric vehicles" has been proposed.